ELSEVIER

Thin Solid Films 358 (2000) 152–158

thin solid films

www.elsevier.com/locate/tsf

Structural characterization and frictional properties of C_{60}-terminated self-assembled monolayers on Au(111)

Seunghwan Lee, Young-Seok Shon, T. Randall Lee*, Scott S. Perry[1]

Department of Chemistry, University of Houston, Houston, TX 77204-5641, USA

Received 8 January 1999; received in revised form 3 July 1999; accepted 3 July 1999

Abstract

C_{60}-terminated self-assembled monolayers (SAMs) were generated on the surface of Au(111) by the adsorption of unsymmetrical disulfides having saturated hydrocarbon backbone structures comprised of six (C-6) and eleven (C-11) carbon atoms. The formation of oriented monolayer films from these adsorbates was confirmed by ellipsometric thickness and contact angle measurements. The morphologies and frictional properties of the C_{60}-terminated SAMs were examined using atomic force microscopy (AFM). The SAMs derived from the C-11 disulfides exhibited smooth morphologies and homogeneous frictional force distributions, which proved ideal for the study of intrinsic frictional properties. The SAMs derived from the C-6 disulfides, however, exhibited rough and inhomogeneous topographic and frictional force distributions. In addition, the shorter SAMs exhibited erratic frictional behavior and partial film delamination. The relative frictional forces observed on these immobilized C_{60} films were higher than those observed on normal methyl-terminated SAMs and on the surface of graphite.

Keywords: Atomic force microscopy; Fullerene; Interfaces; Tribology

1. Introduction

The tribological properties of C_{60} or 'buckminsterfullerene' [1] films have been widely studied because of their potential use as solid lubricants [2–13]. Their structural uniqueness and chemical identity has prompted their comparison to other carbon-based materials such as diamond, graphite, and amorphous carbon [4,10]. Despite the theoretical prediction of exceptional rigidity and load-bearing capacity [14–16], experimental observations of the lubricating properties of C_{60} films have been inconsistent [2–13]. Although low frictional properties of the films have been reported [5–8], the accompanying wear and the mobility of wear debris complicate the characterization of their intrinsic tribological properties. Moreover, many of the C_{60} films reported thus far exhibit 'island' formation due to insufficient coverage [6–9], or exist as multilayers at the other extreme [3,5,10,11]. For the majority of these investigations, the C_{60} films were obtained by sublimation onto various substrates.

To overcome these difficulties, researchers have explored the attachment of C_{60} moieties to the tail groups of self-assembled monolayers (SAMs) [14–19]. Chemical bonding of the C_{60} moieties to the surfaces of SAMs should not only provide discrete monolayers of C_{60}, but also organized assemblies in which the C_{60} moieties will remain immobilized on the surface even when subjected to stress. This approach has been employed in studies of the structural, electrochemical, and biological properties of C_{60} films; its use, however, in the tribological characterization of fullerenes has been somewhat rare [12,13].

We report here the structural characterization and frictional properties of a new class of C_{60} monolayers that are chemically attached to the surfaces of SAMs. Fig. 1 illustrates the nature of these monolayers, which were generated by the adsorption of specifically designed C_{60}-modified unsymmetrical disulfides onto the surface of Au(111) [20]. To explore the relationship between the structure of the underlying saturated hydrocarbon backbones and the frictional properties of the overlying C_{60} layer, we employed two types of disulfides having different chain lengths (C-6 and C-11). We then compared the frictional properties of these SAMs to those of CH_3-terminated SAMs having also C-6 and C-11 chain lengths. Finally, we compared the frictional properties of the C_{60} films to those of the well known solid lubricant graphite (HOPG). With these studies, we

* Corresponding author. Tel.: +1-713-743-2724; fax: +1-713-743-2726.

E-mail address: trlee@uh.edu (T. Randall Lee)

[1] Corresponding author. E-mail address: perry@jetson.uh.edu

0040-6090/00/$ - see front matter
PII: S0040-6090(99)00539-8

wished to determine the influence of immobilization on the tribological properties of well-defined C_{60} monolayer films. Also, we wished to compare the frictional properties of these immobilized C_{60} films with other carbon-based lubricant materials such as normal hydrocarbons and graphite.

2. Experimental

Fig. 1 illustrates the structures of the SAMs examined in this work. Fig. 1a shows the SAM derived from the C-6 symmetrical CH_3-terminated disulfide, $[CH_3(CH_2)_5S]_2$ (left), and its unsymmetrical C_{60}-aziridine-terminated analog, $C_{60}N(CH_2)_6SS(CH_2)_5CH_3$ (right). Fig. 1b shows the SAM derived from the C-11 symmetrical CH_3-terminated disulfide, $[CH_3(CH_2)_{10}S]_2$ (left), and its unsymmetrical C_{60}-aziridine-terminated analog, $C_{60}N(CH_2)_{11}SS(CH_2)_{10}CH_3$ (right). Details of the synthesis of the C_{60}-aziridine-terminated C-6 disulfide have been provided elsewhere [20]. The C_{60}-aziridine-terminated C-11 disulfide was prepared similarly. ^{1}H NMR ($CDCl_3$): δ3.67 (t, $J = 7.7$ Hz, 2 H, NCH_2CH_2), 2.67 (t, $J = 8.0$ Hz, 2 H, SCH_2CH_2), 2.64 (t, $J = 8.0$ Hz, 2 H, SCH_2CH_2), 2.20–2.10 (m, 2 H), 1.81–1.51 (m, 6 H), 1.42–1.5 (m, 28 H), 0.89 (t, $J = 7.7$ Hz, 3 H, CH_2CH_3).

For the thickness and wettability studies, the disulfides were adsorbed onto polycrystalline gold substrates, which were prepared by thermally evaporating gold onto silicon wafers [21]. The thicknesses of the SAM films were measured by ellipsometry using a Rudolf Research Auto EL III ellipsometer equipped with a He—Ne laser (632.8 nm at an angle of incidence of 70°). A refractive index of 1.45 was assumed for all films. The contact angles of water (H_2O) were measured using a ramé-hart model 100 contact angle goniometer. For topographic and frictional studies, the SAMs were obtained by immersing Au(111) surfaces into 10^{-5} M solutions of the unsymmetrical C_{60}-terminated disulfides dissolved in benzene or 10^{-3} M solutions of the symmetrical CH_3-terminated disulfides dissolved in ethanol. The Au(111) surfaces were obtained by annealing a gold wire in a flame of H_2/O_2 to produce a number of atomically flat (111) terraces around the circumference of the microball. Detailed procedures for the preparation and characterization of these gold substrates are available in a previous publication [22].

Topographic and frictional measurements of the SAMs were performed using an atomic force microscope (AFM). The instrument employed here utilizes a conventional beam deflection technique with a single tube scanner (0.5″ in diameter and 1.0″ in length) [22]. In this technique, light from a laser diode is focused on the backside of the V-shaped microfabricated cantilever, which supports the probe tip underneath. In this experimental approach, the sample is scanned relative to a fixed cantilever position. Deflections of the cantilever generated by interaction of the probe tip and the sample surface is detected by a four-quadrant position-sensitive detector. With this approach, both normal and lateral deflections of the cantilever can be simultaneously recorded. Sample positioning as well as data collection and processing were controlled by RHK AFM 100 and RHK STM 1000 electronics and software.

We adopted two different approaches for the studies of friction. In the first approach, the force between the tip and the sample surface was maintained at a constant normal force (zero applied load) using a feedback system while topographic images of the surface were obtained. This approach produced two-dimensional maps of the film topography and the spatial distribution of lateral forces across the film surface. These maps provide information regarding the homogeneity of the films in terms of frictional properties as well as the average frictional forces at zero applied load in a given area.

In the second approach, the feedback control of the normal load between the tip and the surface was disabled, and the sample surface was rastered laterally over the same line (1000 Å scan length) as a function of a systematically varied applied load (maximum of ~30 nN). The lateral forces were then plotted as a function of load to yield a 'friction-load' map [22]. For statistical validity, friction-load maps were obtained from several different areas of the sample surfaces. Normal loads have been expressed in force units (nN) using the manufacturer's (Digital Instruments, CA; 0.58 Nm^{-1}) specifications of the force constant

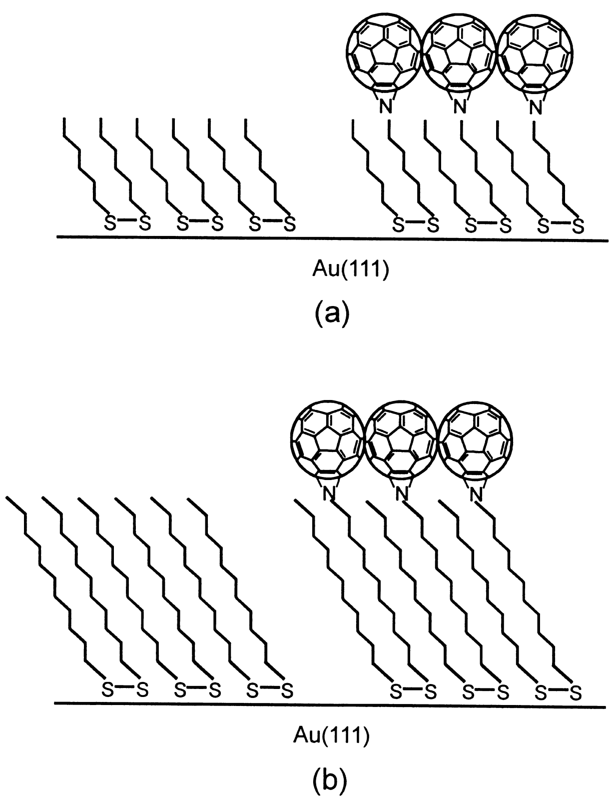

Fig. 1. Illustration of the types of SAMs derived from: (a) the C-6 symmetrical CH_3-terminated disulfide (left) and the C-6 unsymmetrical C_{60}-terminated disulfide (right), and (b) the C-11 analogs, respectively. Note that the overlying C_{60} moieties are depicted as large spheres.

of the cantilever. Lateral forces have been expressed in voltage (V) as measured at the photodetector without further conversion. Several different cantilever-tip assemblies were used in this work for duplicate experiments. All data presented here for the purpose of comparison in the same plot or in the same table, however, were obtained with a single cantilever-tip assembly to ensure validity. The radii of the AFM tips used were ~700 Å, as determined by imaging a standard sample [23].

3. Results and discussion

3.1. Thicknesses and wettabilities of SAMs

Because the van der Waals diameter of C_{60} (~10 Å) is approximately twice the lattice spacing of simple CH_3-terminated SAMs on gold (~5 Å) [20,24–26], the unsymmetrical disulfides employed here represent ideal underlying hydrocarbon moieties for the generation of C_{60}-terminated SAMs on gold (see Fig. 1). Indeed, previous studies by scanning tunneling microscopy (STM) have confirmed that these SAMs expose C_{60} moieties at the interface [20,27]. To further confirm that the hydrocarbon underlayers are substantially covered by C_{60} moieties, we characterized the films by ellipsometry and contact angle measurements. We then compared these data to those of SAMs derived from normal alkanethiols with chain lengths equivalent to those proposed to lie beneath the C_{60} moieties as illustrated in Fig. 1. For the purpose of comparison, we measured contact angles on graphite as well. The results of these studies are summarized in Table 1. Measurements of the ellipsometric thickness of both SAMs derived from the C_{60}-terminated disulfides – 16.5 Å for $C_{60}N(CH_2)_6SS(CH_2)_5CH_3$ and 21.8 Å for $C_{60}N(CH_2)_{11}SS(CH_2)_{10}CH_3$ – showed an approximately 10 Å greater thickness than the SAMs derived from the corresponding normal alkanethiols – 5.5 Å for $CH_3(CH_2)_5SH$ and 13.7 Å for $CH_3(CH_2)_{10}SH$, respectively. Given the probable differences in refractive index of the two types of SAMs as well as possible effects due to optical anisotropy [28], the measured differences in thickness show surprisingly good agreement with the diameter of the C_{60} moieties. These results are thus consistent with the structural model proposed in Fig. 1.

Table 1
Ellipsometric thicknesses (Å) and contact angles of water on SAMs on Au(111)[a]

Samples	Ellipsometric thickness (Å)	Advancing contact angle of water (°)
$CH_3(CH_2)_5SH$	5.5	108
$CH_3(CH_2)_{10}SH$	13.7	114
$C_{60}N(CH_2)_6SS(CH_2)_5CH_3$	16.5	89
$C_{60}N(CH_2)_{11}SS(CH_2)_{10}CH_3$	21.8	87
Graphite	–	86

[a] Average values from multiple independent measurements are reported. Errors in ellipsometric thicknesses are estimated at ±3 Å errors in contact angle values are estimated at ±2°.

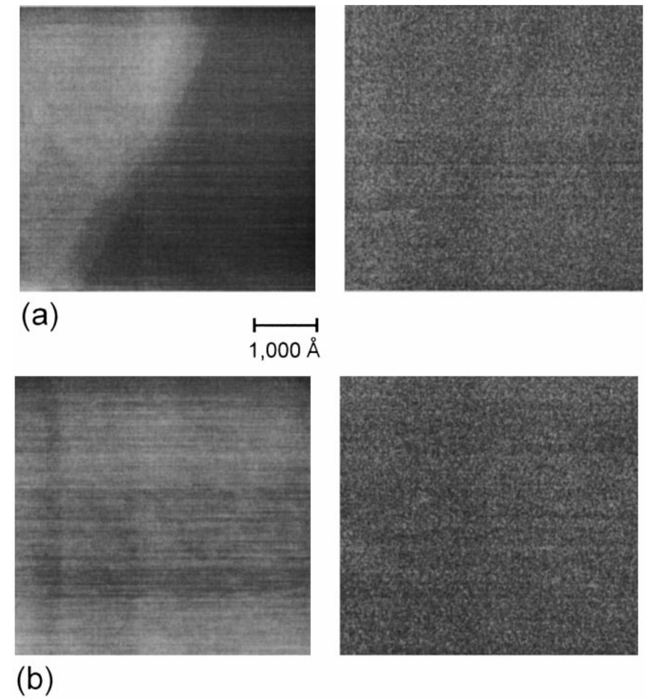

Fig. 2. Topographic (left) and lateral force (right) images of SAMs derived from: (a) the C-6 symmetrical CH_3-terminated disulfide and (b) the C-11 symmetrical CH_3-terminated disulfide. The scale of the image is ~0.5 × 0.5 mm. Enhanced brightness corresponds to increased height in the *z*-direction.

Contact angle measurements provide a sensitive probe of the nature of the terminal functional groups of organic thin films [29,30]. When using water as the contacting liquid (Table 1), both the C-6 ($\theta_a^{H_2O} = 89°$) and the C-11 ($\theta_a^{H_2O} = 87°$) C_{60}-terminated SAMs exhibited slightly higher advancing contact angles than those previously reported for C_{60}-terminated SAMs [15,17,19]. The values are, however, substantially lower than those obtained on SAMs formed from the corresponding normal alkanethiols ($\theta_a^{H_2O} = 108°$ for $CH_3(CH_2)_5SH$ and 114° for $CH_3(CH_2)_{10}SH$). The differences in the advancing contact angles of water on the C_{60}- and CH_3-terminated films appear consistent with the exposure of C_{60} rather than CH_3 moieties at the surfaces of the SAMs formed from the unsymmetrical disulfides. Furthermore, the similar values of the advancing contact angle of water measured on graphite ($\theta_a^{H_2O} = 86°$) and on the chemically similar C_{60}-terminated SAMs ($\theta_a^{H_2O} = 87$–$89°$) provide additional support for this model.

3.2. Topographic and lateral force images of SAMs

Figs. 2 and 3 provide representative AFM images of the SAMs studied in this work. In Fig. 2a, topographic (left) and lateral force (right) images of the SAM formed from the C-6 symmetrical CH_3-terminated disulfide are presented. This

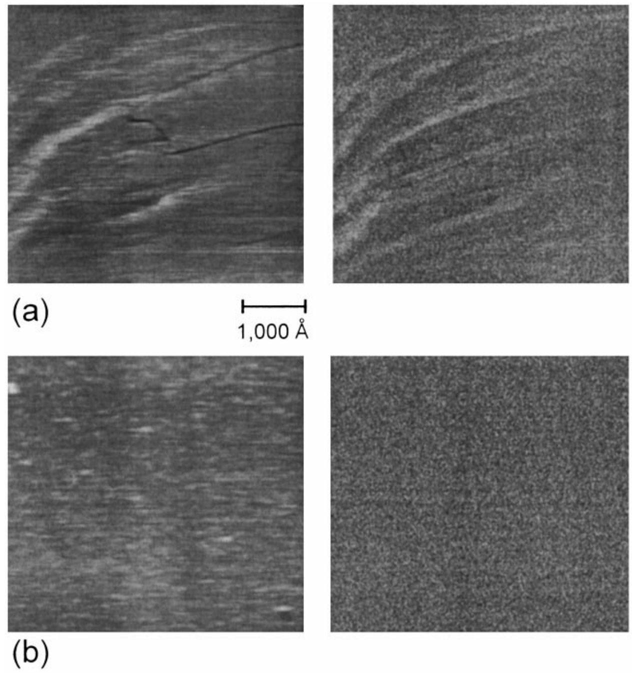

Fig. 3. Topographic (left) and lateral force (right) images of SAMs derived from: (a) the C-6 unsymmetrical C_{60}-terminated disulfide and (b) the C-11 unsymmetrical C_{60}-terminated disulfide. The scale of the image is $\sim 0.5 \times 0.5$ mm. The brighter areas of the topographic and lateral force images correspond to higher topographic features and higher frictional

SAM exhibited a smooth and featureless morphology over the scale shown ($\sim 0.5 \times 0.5$ μm), except for well defined steps and terraces arising from the underlying Au(111) substrate. Enhanced brightness in the images corresponds to increased height in the *z*-direction. Lateral force images yielded a homogeneous distribution of frictional forces over the scanned area. Comparison of both images suggests that topographic features such as steps and terraces exert no influence upon the frictional properties of the film. Smooth morphologies and homogeneous frictional force distributions were also seen on the SAM formed from the C-11 symmetrical CH_3-terminated disulfide (Fig. 2b). Topographic corrugation over the flat areas of both CH_3-terminated films was less than ~2Å.

SAMs formed from the unsymmetrical C_{60}-terminated disulfides, however, exhibited features that varied with the length of the underlying hydrocarbon chains (see Fig. 3a,b). For the SAM derived from the C-6 unsymmetrical C_{60}-terminated disulfide (Fig. 3a), the topographic image (left) was substantially rougher than those of the CH_3-terminated films. The topographic corrugation over the feather-like features (brightest areas), for example, suggested heights of as much as ~20 Å. Furthermore, the lateral force image (right) revealed an inhomogeneous distribution of frictional forces, unlike those of the CH_3-terminated SAMs. Brighter regions in the lateral force images correspond to higher friction. Meanwhile, the topographic image of the SAM derived from the C-11 unsymmetrical C_{60}-terminated disulfide (left image in Fig. 3b) exhibited homogeneously distributed grainy features with underlying terraces. The surface of this film (rms roughness of 4.0 Å per 0.5 μm^2 with height variations of ≤10 Å) appeared much smoother than that of the C-6 unsymmetrical C_{60}-terminated SAM, but rougher than that of the CH_3-terminated SAMs. Furthermore, despite the grainy features seen in the topographic image, the lateral force image (right image in Fig. 3b) exhibited homogeneous frictional force distributions similar to the CH_3-terminated SAMs.

Average frictional forces and the standard deviation of the lateral force images of the SAMs were measured at zero applied load; these measurements, together with those on graphite, are summarized in Table 2. The two CH_3-terminated SAMs exhibited comparable average frictional forces at zero applied load: 42.1 mV for C-6 and 39.0 mV for C-11. Higher average frictional forces were measured on the C-60 terminated SAMs: 113 mV for C-6 and 104 mV for C-11. The frictional properties of all SAMs were substantially higher than that of graphite: 0.7 mV. Although the absolute values of the frictional forces were different for each measurement, the relative magnitudes of these forces on the various samples were reproducible. The standard deviation of lateral force images, which correlates with the homogeneity of the frictional properties, were comparable for all of the SAMs and graphite (except perhaps for the marginally higher value observed for the six-carbon C_{60}-terminated SAM).

From these observations, we conclude that the target material in this work, anchored films of C_{60}, are well formed as SAMs on Au(111) when chemically attached to dialkyl disulfides having relatively long hydrocarbon chains (e.g. C-11). When chemically attached to shorter hydrocarbon chains (e.g. C-6), however, the SAMs are rough and inhomogeneous. These results are unsurprising in light of the known phenomenon that chain lengths of less than 10 carbon atoms yield disordered SAMs from either alkylsiloxanes or alkanethiols [29–31]. We believe that the roughness and inhomogeneity of the shorter C_{60}-terminated films partly arise from deformations induced by the scanning probe tip. When the topography of the six-carbon C_{60}-terminated SAM was measured by STM (i.e. in the absence of mechanical perturbation), a more homogeneous structure

Table 2
Average frictional forces and the standard deviation of the lateral force images at zero applied load obtained on SAMs on Au(111)

Samples	Average friction (mV)	Standard deviation of lateral force images (mV/0.25 μm^2)
$[CH_3(CH_2)_5S]_2$	42.1	15.8
$[CH_3(CH_2)_{10}S]_2$	39.0	16.2
$C_{60}N(CH_2)_6SS(CH_2)_5CH_3$	113	19.3
$C_{60}N(CH_2)_{11}SS(CH_2)_{10}CH_3$	104	17.0
Graphite	0.70	15.4

was observed [20] than is observed here. Although the present AFM images were obtained with zero applied load, there still exist attractive forces between the tip and the films while scanning. These attractive forces might influence the observed structures of the films.

3.3. Friction-load maps of the six-carbon C_{60}-terminated SAM

Friction-load maps measured on the SAM formed from the C-6 unsymmetrical C_{60}-terminated disulfide were obtained from several different areas of the film. Similar to the lateral force image at zero load shown in Fig. 2b, the frictional measurements collected as a function of load were different from area to area, reflecting the inhomogeneous frictional properties across the sample surface and suggesting an inhomogeneous C_{60}-terminated SAM. As a consequence, it would be misleading to offer a single map as representative of these films. We present instead a few notable examples of friction-load maps obtained from several different areas. In the first example, shown in Fig. 4a, nonlinearities or discontinuities in the frictional response are observed at different load regimes and are suggestive of rupture or drastic deformation of the film. While the load regime in which the deformation occurred varied from run to run, the phenomenon was observed in most measurements on these SAMs.

A second example is shown in Fig. 4b, where large fluctuations are observed in the frictional force as a function of load, suggesting that structural changes are occurring as the tip is scanned over the surface of the film. Also, distinctively different slopes of the friction-load maps, which reflect the inherent frictional properties of a material in macroscopic contact [32], were frequently observed on the surface of a single given sample. Insight into these fluctuations and variations was obtained by scanning the tip on the surface of graphite before and after obtaining frictional measurements on the film. As shown in Fig. 5, when the graphite surface was imaged immediately after rastering over the C_{60} film, higher frictional forces were observed than when graphite was scanned first. This observation strongly suggests that material is transferred from the film surface to the AFM tip during the scanning process. We thus conclude that the six-carbon C_{60}-terminated SAM undergoes substantial deformation when in contact with the AFM probe tip in this load regime.

3.4. Friction-load maps of the eleven-carbon C_{60}-terminated SAM

In contrast to the C_{60}-terminated SAM described above, the SAM formed from the C-11 unsymmetrical C_{60}-terminated disulfide showed reproducible frictional behavior as a function of load. Fig. 6 shows the overlap of five different friction-load maps obtained from five different areas of this film. The data show excellent reproducibility and exhibit the anticipated non-linear Hertzian deformation as a function of

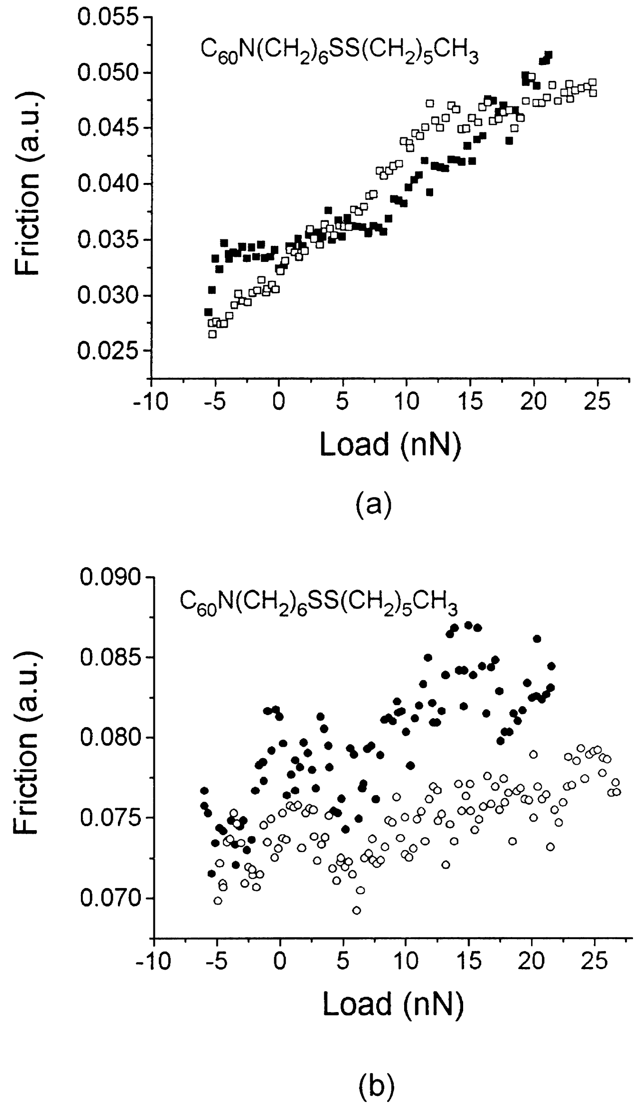

Fig. 4. Friction-load plots obtained on the SAM derived from the C-6 unsymmetrical C_{60}-terminated disulfide illustrating (a) film deformation, as revealed by nonsystematic slope changes in the friction-load curves, and (b) the large fluctuations and varied frictional responses of this film. The filled and unfilled symbols indicate measurements taken from two different regions of the surface.

load ($F_f \sim L^{2/3}$) [33]. Furthermore, the same stable and robust structure shown in Fig. 3b was observed repeatedly when imaged over the area at which the frictional data were collected. No evidence of plastic deformation was observed. Also, no evidence for material transfer was observed as was seen for the six-carbon C_{60}-terminated films (vide supra). The stability of this C_{60} film is attributed to the additional stability afforded by increased van der Waals interactions between the underlying chains (e.g. film stabilization by as much as 0.8 kcal/mol per additional CH_2 has been reported [34]).

The construction of structurally stable and homogeneous C_{60} monolayer films enabled us to investigate the intrinsic frictional properties of immobilized C_{60} moieties without

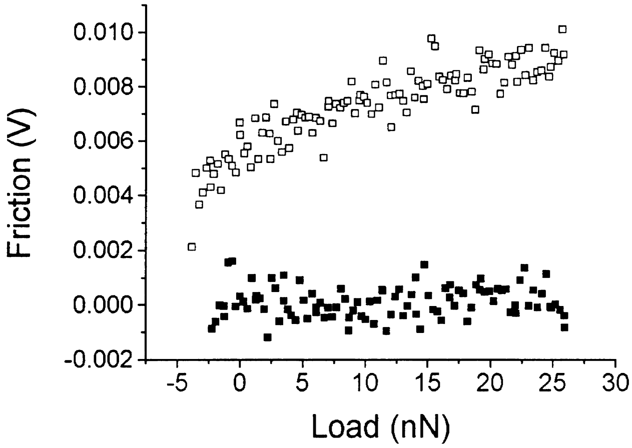

Fig. 5. Friction-load maps obtained on graphite (HOPG) both before (filled) and after (unfilled) scanning on the SAM formed from the C-6 unsymmetrical C_{60}-terminated disulfide.

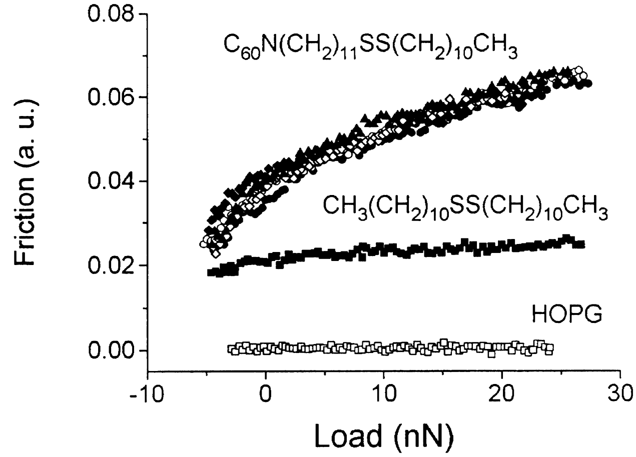

Fig. 6. Frictional-load maps of the SAM formed from the C-11 unsymmetrical C_{60}-terminated disulfide (top), the SAM formed from the C-11 symmetrical CH_3-terminated disulfide (center), and the surface of graphite (HOPG; bottom).

interference from mechanical instability. Fig. 6 compares the frictional properties of the C_{60}-terminated C-11 film to those of the CH_3-terminated C-11 film and graphite. The highest frictional forces were reproducibly observed on the C_{60} film over the entire range of loads employed. Although a quantitative comparison of our results with other previous reports is hampered by differences in instrumental conditions and calibration issues, the observed higher frictional properties of the C_{60} film examined here, when compared to standard materials such as graphite, is consistent with previous reports [4,10] of the relatively poor tribological performance of C_{60} moieties.

3.5. Tribological implications of the results

Examination of the morphological features and frictional properties of the present 'immobilized' C_{60} films provides new insight into the nature of C_{60} as a tribological agent. The data obtained from the C_{60} films with underlying C-11 hydrocarbon chains show substantially higher friction than was observed on the chemically similar surface of graphite. These data therefore suggest that the attractive lubricant properties of C_{60} reported in the literature [5–8] arise, at least in part, from non-chemical sources. We note further that film deformation and material transfer were seen when the C_{60} moieties were attached to the less stable underlying C-6 hydrocarbon chains. From one perspective, these latter C_{60} films might more closely represent the frictional properties of free C_{60} acting as a lubricant. Although a 'micro-bearing' motion has long been predicted to enhance the tribological properties of C_{60}-based lubricants [2–13], our results find no support for this phenomenon.

4. Conclusions

The frictional properties of C_{60} films immobilized on the surface of self-assembled monolayers were investigated using atomic force microscopy. Unsymmetrical disulfides with two different chain lengths, C-6 and C-11, were chosen as templates to provide underlying hydrocarbon backbones for the C_{60}-terminated SAMs. The formation of C_{60}-terminated films was confirmed by ellipsometric thickness and contact angle measurements. Immobilization of the C_{60} moieties on C-11 hydrocarbon underlayers provided homogeneous monolayer films that were ideal for fundamental friction studies; frictional measurements on these films were free from artifacts due to mechanical instability. In contrast, inhomogeneous and/or unstable C_{60} films were produced when C-6 hydrocarbon underlayers were employed. The frictional forces of the former C_{60} films exhibited a well behaved non-linear relationship in response to changes in load, consistent with the model of Hertzian deformation ($F_f \sim L^{2/3}$). Finally, the frictional forces of the well-behaved C_{60} film were higher than those observed on CH_3-terminated films and much higher than those observed on graphite in the load regime adopted in this work (maximum load ~ 30 nN). Our results are thus inconsistent with a model in which C_{60} moieties act as superior lubricating agents.

Acknowledgements

We thank the National Science Foundation for grants DMR-9700662 and CHE-9625003 (CAREER Award to TRL) and the Robert A. Welch Foundation for grant E-1320.

References

[1] H.W. Kroto, J.R. Heath, S.C. O'Brien, R.F. Curl, R.E. Smalley, Nature 318 (1985) 162.

[2] S. Hoen, N.G. Chopra, X.-D. Xiang, R. Mostovoy, Jianguo Hou, W.A. Vareka, A. Zette, Phys. Rev. B 46 (1992) 12737.
[3] T. Thundat, R.J. Warmack, D. Ding, R.N. Compton, Appl. Phys. Lett. 63 (1993) 891.
[4] C.M. Mate, Wear 168 (1993) 17.
[5] B. Bhushan, B.K. Gupta, G.W. Van Cleef, C. Capp, J.V. Coe, Appl. Phys. Lett. 62 (1993) 3253.
[6] R. Lüthi, E. Meyer, H. Haefke, L. Howald, H.-J. Güntherodt, Helv. Phys. Acta 67 (1994) 755.
[7] R. Lüthi, E. Meyer, H. Haefke, L. Howald, W. Gutmannsbauer, H.-J. Güntherodt, Science 266 (1994) 1979.
[8] R. Lüthi, E. Meyer, H. Hafke, L. Howald, W. Gutmannsbauer, M. Guggisberg, M. Bammerlin, H.-J. Güntherodt, Surf. Sci. 388 (1995) 247.
[9] U.D. Schwarz, W. Allers, G. Gensterblum, R. Wiesendanger, Phys. Rev. B. 52 (1995) 14976.
[10] U.D. Schwarz, O. Zworner, P. Koster, R. Wiessendanger, Phys. Rev. B. 56 (1997) 6987.
[11] G. Luengo, S.E. Campbell, V.I. Srdanov, F. Wudl, J.N. Israelachvili, Chem. Mater. 9 (1997) 1166.
[12] L.M. Lander, W.J. Brittain, V.A. DePalma, S.R. Girolmo, Chem. Mater. 7 (1995) 1437.
[13] V.V. Tsukruk, M.P. Everson, L.M. Lander, W.J. Brittain, Langmuir 12 (1996) 3905.
[14] W.B. Caldwell, K. Chen, C.A. Mirkin, S.J. Babinec, Langmuir 9 (1993) 1945.
[15] K. Chen, W.B. Caldwell, C.A. Mirkin, J. Am. Chem. Soc. 115 (1993) 1193.
[16] J.A. Chupa, S. Xu, R.F. Fischetti, R.M. Strongin, J.P. McCauley Jr., A.B. Smith III, J.K. Blasie, J. Am. Chem. Soc. 115 (1993) 4383.
[17] V.V. Tsukruk, L.M. Lander, W.J. Brittain, Langmuir 10 (1994) 996.
[18] X. Shi, W.B. Caldwell, K. Chen, C.A. Mirkin, J. Am. Chem. Soc. 116 (1994) 11598.
[19] L.M. Lander, W.J. Brittain, E.A. Volger, Langmuir 11 (1995) 375.
[20] Y.-S. Shon, K.F. Kelly, N.J. Halas, T.R. Lee, Langmuir 15 (1999) 5329.
[21] Y.-S. Shon, T.R. Lee, Langmuir 15 (1999) 2236.
[22] H.I. Kim, T. Koini, T.R. Lee, S.S. Perry, Langmuir 13 (1997) 7192.
[23] S.S. Sheiko, M. Moller, E.M.C.M. Reavekamp, H.W. Zandbergen, Phys. Rev. B 48 (1993) 5765.
[24] E.I. Altman, R.J. Colton, Surf. Sci. (1992) 279.
[25] E.I. Altman, R.J. Colton, Surf. Sci. 295 (1993) 13.
[26] C.E. Chidsey, D.N. Loiacono, Langmuir 6 (1990) 682.
[27] K.F. Kelly, Y.-S. Shon, T.R. Lee, N.J. Halas, J. Phys. Chem. B (1999) in press.
[28] V.K. Gupta, N.L. Abbott, Langmuir 12 (1996) 2587.
[29] C.D. Bain, E.B. Troughton, Y.-T. Tao, J. Evall, G.M. Whitesides, R.G. Nuzzo, J. Am. Chem. Soc. 111 (1989) 321.
[30] M.D. Porter, T.B. Bright, D.L. Allara, C.E.D. Chidsey, J. Am. Chem. Soc. 111 (1989) 3559.
[31] J. Ruhe, V.J. Novotny, K.K. Kanazawa, T. Clarke, G.B. Street, Langmuir 9 (1993) 2382.
[32] F.P. Bowden, D. Tabor, The Friction and Lubrication of Solids, Clarendon Press, Oxford, 1986.
[33] K.L. Johnson, Contact Mechanics, Cambridge University Press, Cambridge, 1985.
[34] R.G. Nuzzo, L.H. Dubois, D.L. Allara, J. Am. Chem. Soc. 112 (1990) 558.